Paper for COCIS (X-ray & Neutron Scattering Section)

Combining wide-angle and small-angle scattering to study colloids and self-assembly

Karen J. Edler[a*] and Daniel T. Bowron[b]

a. Department of Chemistry, University of Bath, Claverton Down, Bath BA2 7AY, k.edler@bath.ac.uk
b. ISIS, Science and Technology Facilities Council Rutherford Appleton Laboratory, Harwell Oxford, Didcot OX11 0QX, UK, daniel.bowron@sftc.ac.uk

* corresponding author

Abstract

The characterization of structure over a wide range of length scales from atomic to microns is a common requirement for understanding the behaviour of many soft matter systems. In the case of self-assembling and colloidal materials, the final properties will depend sensitively on intermolecular as well as interparticle interactions. Experimental methods such as wide and small angle scattering, which, between them, cover a wide range of length-scales are therefore growing in importance to better understand and thus exploit these systems. This review covers the growing use of wide angle scattering, either in conjunction with small angle scattering, or applied to systems which have previously been studied using small angle scattering, in order to highlight the complementarity between these two techniques, and the areas where atomistic information has contributed to understanding of the behaviour of systems containing structure at much larger length scales.

Keywords: small angle scattering; wide angle scattering; colloids; surfactants; amphiphiles; self-assembly; mesostructure; solutions

Graphical Abstract

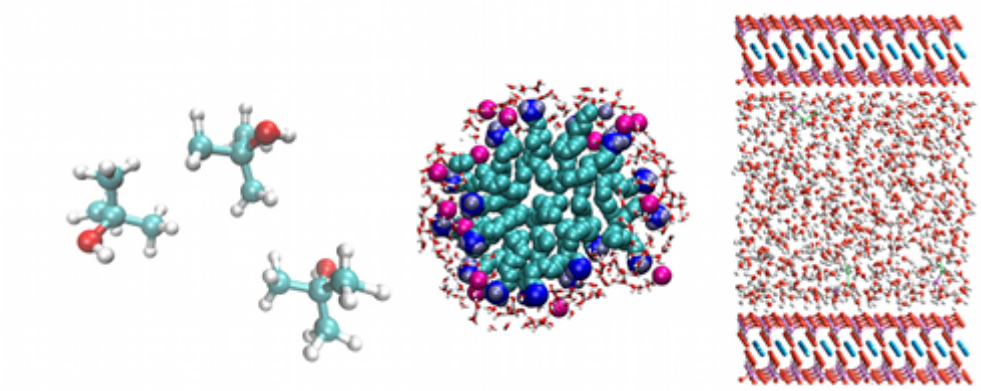

1. Introduction

Small and wide-angle neutron scattering are each separately well-established techniques for characterization of solution structures. Small angle neutron scattering (SANS) measures structures in a size range from roughly 1 nm to several hundreds of nm, depending on the angle range measured.[1-2] It is widely used in the study of a range of colloidal systems from nanoparticles, to micelles and biomolecules in solution. Wide-angle neutron scattering, on the other hand, measures the correlations between molecules in solution on length scales similar to that of crystallography, giving atomic level descriptions of average molecular arrangements within the fluid. Typically wide-angle scattering has seen greater application in the study of molecular liquids, solvation shells and glassy materials, but it is increasingly being used to study more complex molecules and molecular assemblies. Increases in computational power have enabled modeling of larger systems containing bigger molecules or aggregations of molecules, leading to the ability to analyse experimental results covering wider length scales, up to, and now matching to some degree, those sizes typically covered by the small-angle scattering technique. The two techniques are complementary, and potentially overlap in their descriptions of structure, but until recently there has been very little intersection in their application to colloidal and self-assembled systems.

In this review we discuss the recent application of both SANS and wide-angle scattering to a range of materials that has developed over roughly the last twenty years. We have restricted our discussion to systems that do not contain crystalline ordering, as studies of systems showing crystalline or liquid crystalline diffraction peaks alongside nanostructural features are not uncommon. We focus instead on liquid and disordered particulate systems, which do not have strong diffraction features in either wide or small angles. We aim to highlight the complementarity between wide and small angle scattering and demonstrate how a multi-length scale structural understanding of complex soft matter systems can be obtained which enables better insights into function and properties than either technique would alone.

2. Techniques & Theory

In scattering techniques the intensity and shape of the scattered signal arises from density differences in the sample.[1-2] In the case of neutron scattering, since neutrons interact with atomic nuclei, the scattering pattern reflects the distribution of different isotopes within the sample as well as their physical arrangement in space. In the discussion that follows, the

scattering from a sample is measured as a function of Q, the magnitude of the momentum transfer vector of the scattering process. This is defined as:

$$Q = \frac{4\pi}{\lambda}\sin\theta \qquad (1)$$

where λ is the wavelength of the neutron incident upon the sample, and 2θ is the scattering angle.

In small angle scattering, the length scales measured are much larger than individual molecules. Therefore average material properties can be used when analyzing the data. The physical density and the neutron scattering length for the elements in the sample are therefore combined in the scattering length density, *Nb*:

$$Nb = \frac{N_A \cdot \rho}{MW} \sum_i b_i \qquad (2)$$

where ρ is the mass density, MW is the molecular weight and b_i the neutron scattering length for the isotopes present. For small angle scattering from colloids or self-assembled micellar or lipid systems, the data is usually modeled in terms of objects with defined shape (e.g. sphere, cylinder, core-shell ellipsoid), interacting with each other in a solvent (Figure 1). A collection of such models can be found in reference 3. Scattering length densities can therefore be calculated for the shape, or regions of the shape in the sample (eg for a nanoparticle or for the solvent). The shape term is designated the form factor ($F(Q)$), while interactions between objects are described by the structure factor ($S(Q)$). For a system containing monodisperse, spherically-symmetric particles, the scattered intensity I(Q) can then be expressed as:

$$I(Q) = N_p V_p^2 (Nb_p - Nb_s)^2 F(Q) S(Q) + B_{inc} \qquad (3)$$

where N_p is the number of particles, V_p is the volume of the particles , Nb_p and Nb_s are the scattering length densities of the particle and solvent respectively, while B_{inc} is the incoherent background scattering. More complicated approaches are needed for polydisperse and/or non-spherosymmetric particle systems.[4] SANS is a low-resolution technique since a typical measurement will span roughly a Q range of 0.007 to 0.3 $Å^{-1}$, meaning that molecular details cannot be resolved.

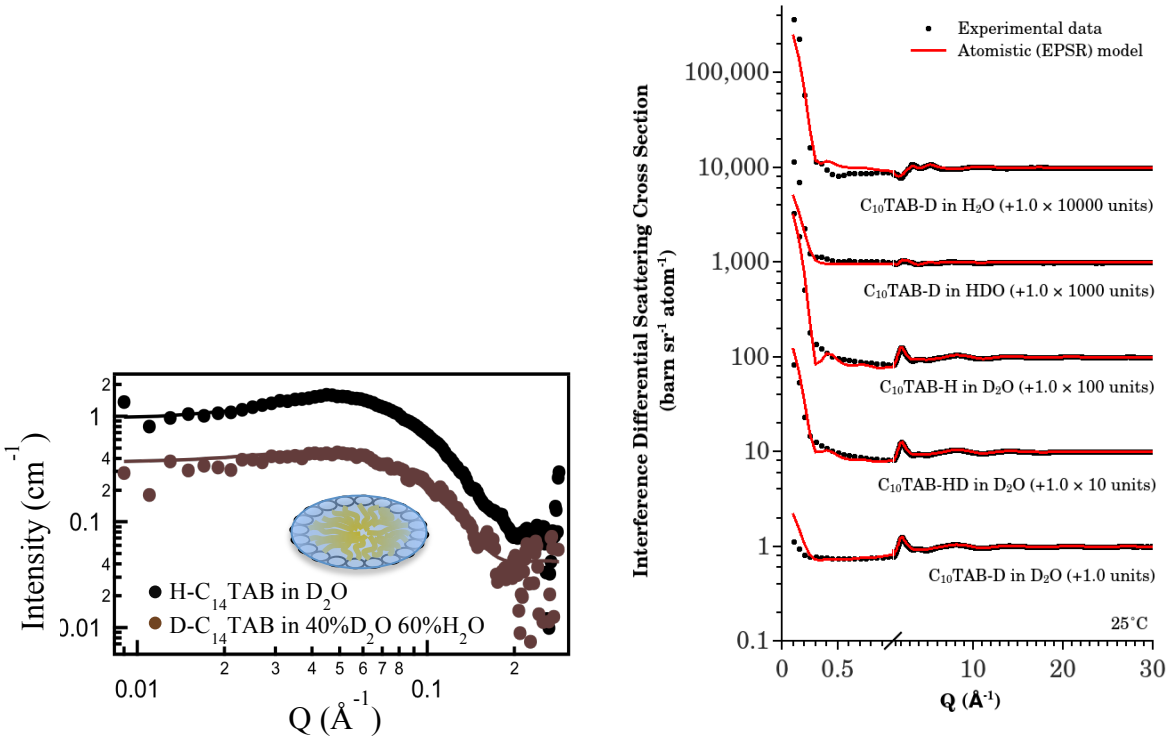

Figure 1: (left) Example of small angle scattering data from 0.037M tetradecyltrimethylammonium bromide micelles in water in the presence of the water soluble polyelectrolyte polyethylenimine (M_w ~2000, 3wt%), fitted to a low resolution uniform ellipse model, with a repulsive charged-sphere structure factor[5] (right) Wide angle scattering data from multiple neutron contrasts fitted to an atomistic model of surfactant molecules in water, arranged into micelle clusters as shown in Figure 3.

In contrast to the case of small angle scattering, wide angle scattering from liquids or non-crystalline systems is typically measured over a Q-range from ≤ 0.1Å^{-1} to ≥ 20 Å^{-1}, and consequently probes structural correlations in the sample with atomic resolution or better. The experiments themselves measure the total structure factor, *S(Q)*, which is defined via the atomic structure as:[6]

$$S(Q) - 1 = \frac{1}{(\sum_\alpha c_\alpha \langle b_\alpha \rangle)^2} \sum_\alpha \sum_{\beta \geq \alpha} (2 - \delta_{\alpha\beta}) c_\alpha c_\beta \langle b_\alpha \rangle \langle b_\beta \rangle [S_{\alpha\beta}(Q) - 1] \qquad (4)$$

c_α and c_β are the atomic concentrations of atoms of type α and β in the sample, and $\langle b_\alpha \rangle$ and $\langle b_\beta \rangle$ are the corresponding bound coherent scattering lengths of the atomic elements or if appropriate, their isotopes. $S_{\alpha\beta}(Q)$ are the Faber-Ziman partial structure factors[7] describing the pair correlations between atoms of type α and β, and $\delta_{\alpha\beta}$ is the Kronecker delta function to avoid double counting the like-atom correlations.

As the experiment is atomistic in nature there is no need to include a form factor to encode particle shapes within the measured total structure factor, and instead data is generally analyzed in terms of the related total radial distribution function, *G(r)*. This is obtained from the structure factor via the well-known Fourier transform:

$$G(r) - 1 = \frac{1}{(2\pi)^3 \rho_0} \int_0^\infty 4\pi Q^2 (S(Q) - 1) \frac{\sin Qr}{Qr} dQ \qquad (5)$$

ρ_0 is the atomic density of the sample. The total pair distribution function is formed from the sum of the Faber-Ziman atomic site-site partial pair distribution functions, $g_{\alpha\beta}(r)$, in the same way as the total structure factor is formed from the partial structure factors in Equation (4).

As wide angle scattering is atomistic in nature, the scattering signal from samples formed from more than one type atom is inherently complex, containing $N(N+1)/2$ partial pair correlations, where *N* is the number of atomic components. This means that interpreting the experimental data is, more often than not, a significant challenge. Thankfully, modern computational resources, combined with physico-chemically constrained atomistic modeling methods now make it possible to construct detailed three-dimensional models of structurally disordered systems. These models are built to satisfy the essential criterion that the final atomic and molecular configurations are consistent with available neutron or X-ray scattering data[8-9] (Figure 1). The models then provide access to the partial atomic pair correlation functions, $S_{\alpha\beta}(Q)$ and $g_{\alpha\beta}(r)$, that are frequently the primary target of structural studies.[10]

Where such computational methods have been applied to the investigation of molecular liquid systems, the technique of Empirical Potential Structure Refinement (EPSR)[9-10] has proven to be the most effective and widely adopted approach. This method effectively generates an ergodic simulation of a liquid system based on pairwise classical interaction potentials operating between the atoms and molecules within the model. The ensemble average of the finite structural realizations thus generated, ultimately reflects the time-average structure of the real system.

Worldwide there are now many facilities available for small angle neutron scattering studies, however the number of instruments currently used to measure the wide angle scattering patterns from liquids and nanoscopic objects in solution is much smaller. In the past, wide-angle liquid diffractometers did not extend data collection to the small angle scattering region, and data from small angle scattering instruments was seldom analysed beyond 0.6 $Å^{-1}$, where molecular structure becomes important, except in cases where crystalline diffraction peaks were observed. More recently the collection of wider angle scattering data on SANS

instruments (at least out to 1 $Å^{-1}$) has become frequently routine,[11] whilst the development of pulsed spallation neutron sources such as the ISIS Facility at the Rutherford Appleton Laboratory, Oxfordshire, UK, has allowed us to take this concept much further. The wide-spectral range and wavelength resolution of short-pulse neutron sources, combined with the time-of-flight instrument geometry, has facilitated the development of instruments that can deliver continuous coverage for structure factor measurements over exceptionally large Q-ranges. For example, the SANDALS instrument[12] on the ISIS 50Hz target station is optimized to collect data over a Q range of 0.1 $Å^{-1}$ – 50 $Å^{-1}$, whilst the NIMROD diffractometer[13] on the ISIS 10Hz target station can, under optimal conditions, collect data over a Q range of 0.01 $Å^{-1}$ – 100 $Å^{-1}$. Between these two instruments it is thus possible to collect atomic resolution pair correlation data on disordered systems to length scales of ~30Å and ~300Å respectively. Data collection and data analysis times, which are both longer for the higher resolution data, mean that small angle scattering will remain in high demand for soft matter studies, however in the future many more studies across length scales, from molecular to nanoscopic, can be expected as data analysis techniques are developed to make use of the wider range of data that can be collected.

3.1 Clustering and sub-micellar aggregation of small amphiphiles in solution

Although the traditional approach to study the nanoscale structure of colloidal systems has been to use small angle scattering techniques, the ongoing development of atomistic modeling methods that refine their results against wide angle neutron and X-ray scattering data is beginning to open new and exciting avenues of investigation. These new approaches offer a complementary and structurally higher resolution viewpoint of the atomic and molecular organization in these systems that are characterized by their complex hierarchical structure over several length scales. In effect the scattering data enables the models to evolve and organize themselves on the nanoscale in a manner that is thought to be a reasonable approximation of the way that real self-assembly processes occur in nature.

An early example of this type of investigation can be found in a study of the temperature dependent association and dissociation of tertiary butanol in water at a concentration of 0.04 mole fraction alcohol.[14] At the time the study was performed, the capabilities of the atomistic structure refinement technique had not been extensively explored for investigating molecular aggregation processes on length scales beyond the near molecular neighbour correlations. Some of the primary concerns related to whether a model refined using data of atomistic

resolution and using relatively short-range interatomic potentials, ranging to a maximum distance of 12Å, would be able to capture longer-range structural phenomenology in the system. Consequently the behavior of the resulting models was benchmarked against a traditional small angle scattering study that had unambiguously established a temperature driven association and dissociation process of the alcohol molecules in the solution. Figure 2 shows, as a function of solution temperature, the behavior of the water hydration shell of the tertiary butanol molecules in the distance range from 6.5Å to 9.5Å from the tertiary carbon of the alcohol molecule, and the figure highlights the role of dehydration of the non-polar regions of the amphiphilic alcohol molecule in this distance range at the temperature of maximum association in the solution.

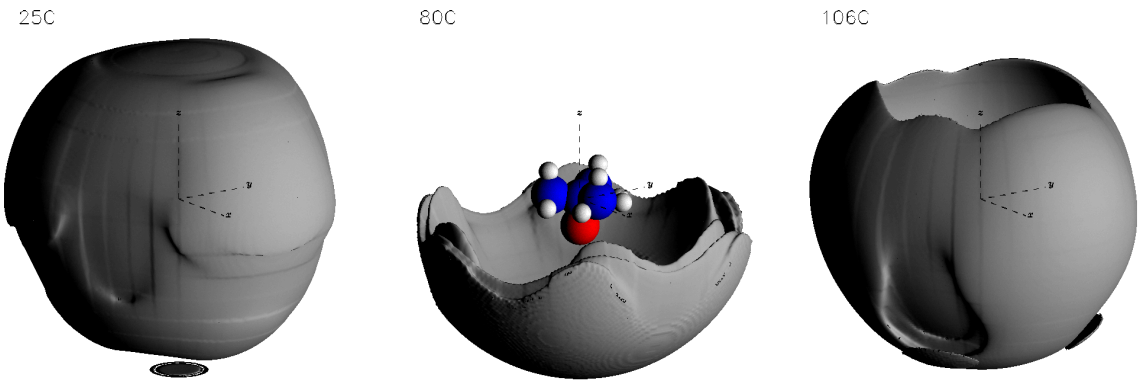

Figure 2: Spatial density functions showing the preferred hydration regions of tertiary butanol molecules in a 0.04 mole fraction aqueous solution as a function of temperature: from left to right, 25°C, 80°C and 106°C. The surfaces show the 30% most favourable probability regions for finding a solvent water oxygen atom around the tertiary-carbon site of the alcohol molecule at the origin in the shell distance range from 6.5Å to 9.5Å.

This result on temperature driven molecular association of tertiary butanol in water is an example of the power of an atomistic modeling approach and follows on from the early successes of the method. In the earlier work, investigating the structure of binary solutions of small amphiphilic molecules (methanol) in water, it was demonstrated that the unusual physical properties of these solutions were related to the underlying mixing state of the solutions on molecular length scales,[15-20] as opposed to commonly espoused clathrate-like hydration structures that have been frequently postulated as the driving force of the unusual thermodynamics of these mixtures.[21]

Naturally, this propensity for binary mixtures of amphiphiles in water to segregate themselves such that the individual molecular components are more likely to find themselves in local environments more comparable to their pure liquids can, in the extreme of water poor solutions, result in aggregation of the water molecules into small pockets within a dominant amphiphilic solvent environment, for example in the tertiary butanol rich[22-23] and sorbitol rich aqueous mixtures.[24]

Although the demixing phenomenology has been found to be very common within binary liquid mixtures, this is not to say that the propensity for molecular length scale separation is necessarily robust when additional components are added to the solutions. An example of this can be seen in the effect of adding the largely non-polar cyclohexene molecule into the concentrated tertiary butanol-water solutions,[25] where the resulting tri-molecular liquid mixture displays more homogenous mixing of all three components in the solution. This is a very important consideration to bear in mind if the structural characterization of the solvent is being pursued to improve our understanding of chemical reaction processes that take place in the media. These cases invariably involve the inclusion of additional solute species and care must therefore be taken to also account for further effects on solvent structuring.

3.2 Case of no self-assembly

In addition to the many studies aimed at clarifying the meso-structure of binary, or more complex aqueous solutions, the atomistic insight obtained from wide-angle neutron scattering measurements has also been extensively used to probe the structure in many room temperature ionic liquids e.g. [26-28] This interesting class of liquid has the potential for very wide novel chemistry and chemical engineering applications, and consequently has attracted significant levels of research interest in the past decade. One particularly intriguing suggestion for the molecular organization in these systems had been that the pure liquids could spontaneously develop meso-scale inhomogeneities due to nanoscale segregation of their molecular components into ionic and non-polar domains, in a manner reminiscent of the formation of micelles in aqueous solutions.[29] In testing this hypothesis, detailed neutron scattering investigations of these systems highlighted that micellar mesostructuring in the liquids does not play a significant role, and that periodic alternating charge ordering of the molecular ions is the dominant interaction motif.[30] In protic ionic liquids this periodic charge ordering can lead to a nanostructure that is more reminiscent of a well dispersed microemulsion or disordered sponge phase.[28] This extended nanostructure, that is periodically

concomitant with the size of the molecules in the liquid, can then play an interesting role when additional solutes are added to the ionic liquid, for example the addition of water to protic ionic liquids has been found to adjust the charge-ordered molecular arrangement to modify its distribution from a reasonably uniform distribution to one where there is some evidence of a branching network of higher curvature.[31]

4. Solution Self-Assembly of Larger Amphiphiles

Small angle scattering (SAS) is widely used to study self-aggregation phenomena of larger molecules, containing both hydrophobic and hydrophilic components, in water. In particular the structure and composition of surfactant micelles, phospholipid bilayers and the interaction of such species with solvents, ions and polymers are a long-standing focus of scattering techniques. Although average properties of the aggregates in these solutions can be obtained using SAS, the details of small molecule binding and water structure around these aggregates is now also starting to be probed by complementary wide-angle scattering measurements.

In molecular biology, dimethylsulfoxide (DMSO)-water solutions interacting with lipid bilayers are known to have a cryoprotective effect, as well as enhancing cell fusion and drug penetration across the skin, with the effect most pronounced for certain DMSO-water concentrations. Small angle scattering and other studies of phospholipid bilayers and vesicles suggest an increase in lipid headgroup area and a dehydration of inter-bilayer space in the presence of DMSO but are equivocal on the extent and position of DMSO binding to the bilayer.[32-34] Wide angle scattering measurements[35] were therefore used in conjunction with molecular dynamics simulations[36] to probe water-DMSO interactions in a 30% solution of DMSO in water near 1,2-dipropionyl-*sn*-glycero-3-phosphocholine (C3-PC). The experimental data indicated that water-DMSO interactions are increased in the presence of the C3-PC phospholipid model. This suggests a possible mechanism for the cryoprotective properties of DMSO-water solutions at this concentration, due to tighter binding of water to DMSO preventing crystallization. It also provided an indirect mechanism for bilayer dehydration suggesting water is pulled out of interbilayer gaps to interact with the DMSO. DMSO also replaced some of the hydrogen-bonded water shell around the nitrogen part of the PC headgroup with the O from DMSO closer to the nitrogen than the water oxygens and the molecule oriented such that methyl groups were further away, and S=O group pointing towards the nitrogen – a possible cause of the observed expansion of headgroup area in phospholipid bilayers in the presence of DMSO. Around the phosphate part of the PC

headgroup the DMSO replaced part of the water but could not H-bond directly to the headgroup so there was no ordering to the DMSO, however a coordinated shell of DMSO formed further out than the first water layer around the headgroup. Possibly the water formed a bridge between phosphate, the area of concentrated DMSO in the outer shell and the DMSO bound to the nitrogen, forming a concentration of methyl groups which favours pockets of hydrophobic species close to the phospholipid headgroup, promoting penetration of the hydrophobe at the surface of a bilayer.

In other small amphiphile systems, wide-angle scattering has been used to compare nanoscale clustering in aqueous solutions of guanidinium carbonate and guanidinium chloride.[37] Guanidinium salts are used to induce protein unfolding in solution, in a process that can be made reversible via careful control of conditions, and thus is of use in a range of biological studies. The structures of guanidinium salt solutions have therefore been extensively studied in attempts to explain this behavior. Simulations predicted that almost all the ions in the carbonate solutions would ion-pair and condense into clusters in solution, and wide-angle scattering data appears to show the presence of extensive ion-pairing in the carbonate solutions, but a much lesser degree in guanidinium chloride solutions. Small angle neutron scattering was used to confirm the presence of clusters with a diameter of the order of 1.6nm in the guanidinium carbonate solutions, and a lack of observable nanoscale structure in the equivalent chloride solutions.[37] The existence of such clusters in solution however is disputed by others using dielectric relaxation spectroscopy, electrical conductivity and the apparent molar volumes of guanidinium carbonate and guanidinium chloride solutions.[38] This system would make a good candidate for further investigation using a neutron scattering instrument that can simultaneously measure both the wide and small angle scattering to help resolve the extent and nature of structuring in these solutions.

In contrast, in a separate set of experiments the structures formed by a series of amino acids in water were studied. Both SANS and wide-angle scattering studies were carried out on the same solutions and although the formation of larger transient clusters of proline[39-40] and glutamine[41] were observed during modeling of the wide angle scattering data and in MD simulations, no larger scale structures were found in the SANS data.

Wide-angle scattering has however now been successfully applied to larger amphiphilic molecules where micellization is well-known and extensively studied. Decyltrimethyl ammonium bromide (C_{10}TAB) is a member of a series of surfactants with a quaternary ammonium headgroup commonly used for several decades in studies of micelle formation

and behavior under a variety of conditions. Members of this class of cationic amphiphiles are commonly used in a range of applications including in antibacterial cleaning fluids, hair conditioners, clothing softeners and as the sacrificial organic templates in the formation of ordered mesoporous silicas. The templating of silica by quaternary ammonium surfactants is thought to depend largely upon interactions between the silica anions, the counterion to the surfactant and H^+ or OH^- binding to the nitrogen containing headgroup (depending on the pH used for the mesoporous silica synthesis).

The water structure around C_{10}TAB headgroups in micelles was therefore the focus of an initial study using wide-angle scattering combined with Empirical Potential Structural Refinement (EPSR) techniques.[9-10] This molecule was chosen since the headgroup is typical of this important series of surfactants, but the C_{10} tail, while long enough to promote micellisation under ambient conditions, contains a relatively low number of atoms to assist in simulating the data. C_{10}TAB is also available in fully deuterated and tail-deuterated forms, providing additional contrasts in H_2O/D_2O solutions to generate multiple scattering curves from solutions differing only in the distribution of the hydrogen/deuterium isotopes. By refining an initial disordered configuration against the set of experimental scattering data a complete atomistic structural picture of the micelles in solution was obtained[42] (Figure 3). The micelle characteristic aggregation number of around 44.5 molecules, counterion dissociation of ~0.3 and diameter of roughly 34 Å diameter corresponded well to that observed for C_{10}TAB micelles characterized using other techniques.[43-45] The extent of counterion dissociation, in particular, matched the expected value of 0.36, calculated using the dressed micelle model.[46]

The data also demonstrated that considerable detail about the water and counterion binding at the micelle surface and the distribution of counterions, headgroups and solvent within the micelles (Figure 3) could be derived using this technique. Strong orientation of the water oxygen atoms relative to the changed nitrogen in the surfactant headgroup was shown to occur and the number of waters per surfactant molecule hydrating the micelle-sized clusters was around 21. The bromide counterions at the micelle surface were also found to retain their hydration shell (6.1 in the first coordination shell compared to 6.3 found for bromide ions in bulk solution), sitting just outside the surfactant headgroups. Disorder in the position of the surfactant headgroups lead to a relatively broad distribution of nitrogen and bromide positions at the micelle surface, with a width at half maximum in the atomic distribution profiles of around 7.4 Å. Although water penetrated into the micelle, it did not penetrate more deeply

than the bromine counterions (likely as their hydration shell), leading to a dry core of around 10 Å radius. Such information is not easily available from other experimental data and gives new insights into micelle structure, and demonstrates the potential to obtain new details of binding to micelles by polyions, hydrophobic species, hydrotropes and complex counterions which will be expanded upon in future experiments.

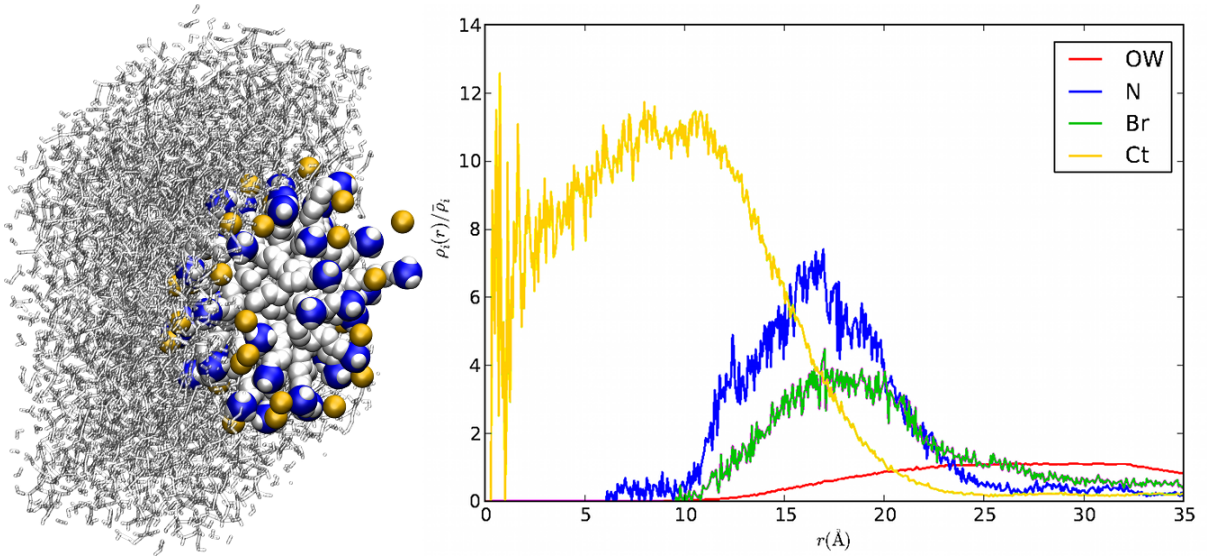

Figure 3: The left panel shows a 43 surfactant ($C_{10}TA^+$) micelle that self-assembled during the structure refinement of wide Q-range neutron scattering data measured for a 0.4M solution of decyltrimethylammonium bromide in water. The initial configuration for the model consisted of a uniform distribution of surfactant monomers, water molecules and bromide counter ions within the simulation box. The graph to right shows the atomic distribution profiles calculated from the centers of mass of micelle structures consisting of 10 surfactant monomers or more, as the modelling process was performed. The atom labels correspond to water oxygen atoms (OW), nitrogen atoms in the surfactant headgroup (N), bromide counter ions (Br), and carbon atoms at the end of the surfactant tails (Ct).

In addition to self-assembled micellar structures, wide-angle scattering has now also been used to study water structures in a water-in-oil emulsion,[47] again using EPSR to develop a fully atomic description of the water-oil interface. Typically such emulsions have been studied using small angle scattering, which gives information on the size and shape of the dispersed phase, but little information on the arrangement of molecules within each phase. A 2:1 water/methylcyclohexane emulsion was studied at very low concentrations of sorbitan tristearate, the stabilizing surfactant – a simplified system to demonstrate the capabilities of the wide angle scattering technique. This composition was selected so that not every water molecule was bonded with the surfactant whereas the opposite was true for the oil phase,

enabling studies of the effect of confinement in the emulsion on the water structure in this phase. Although the water droplets dispersed in the oil had diameters of order of microns it was possible to select the composition, size and shape of the simulation box so that a realistic area of the water-oil interface was modeled with the correct proportions of water to oil to surfactant. The results indicated that the water molecules in the emulsion droplets were on average closer to each other, forming shorter H-bonds. However in addition the relative orientations of the water molecules and their H-bond network were more disordered or distorted, compared to bulk water. The number of nearest neighbor water molecules was higher than in bulk water, (5.5 ± 1.4 within 3.4 Å compared to 4.65 in bulk water) while the angle distribution between three oxygens in the emulsified water phase showed peaks at both the expected tetrahedral angle of 104º but also strongly at 54º, an angle previously associated with interstitial molecules in the first neighbor shell or two interpenetrating, almost tetrahedral networks.[48] This greater disorder may explain phenomena such as the lowering of the water freezing point in emulsions, where liquid water can persist down to 260K.

5. Particulate Self-assembled Structures

In addition to the amphiphile and emulsion systems described above, wide-angle scattering has also been used to probe water structuring and its effect on the properties of particulate structures such as suspensions of inorganic nanoparticles and the self-assembled phases formed by clay particles in water. The high resolution structure of an electrical double layer on clay particles was first reported in 1998,[49] based on studies of a system composed of highly oriented vermiculite gels containing deuterium labelled propylammonium counterions: $C_3H_7NH_3^+$ and $C_3D_7NH_3^+$. Such alkylammonium vermiculite gels provided a good model system to test predictions of electrical double layer structure due to their well-characterized inter-layer separation, which is proportional to the inverse of the square root of the ionic strength. Thus they behave as an ideal 1D colloid at temperatures below their transition temperature to a crystalline state, which occurs at 14ºC. Simultaneous fitting of wide angle scattering data from propylammonium vermiculite gels at the two contrasts demonstrated that the counterions were not tightly bound to the clay surface as suggested by the original model of the Stern layer. Instead they were located in the middle of the inter-layer spacing between clay sheets, separated by two layers of disordered water molecules from the clay surface. The propylammonium groups did not aggregate but were dispersed along this axis despite their relative hydrophobicity. Although the molecular nature of the solvent was important in determining the properties of the electrical double layer close to the surface, there was also no

evidence of surface-induced ordering of the water more than two molecular diameters from the surface.

In contrast a recent study of the water ordering near Laponite particles in aged gelled and young liquid aqueous suspensions demonstrated long-range water ordering did occur in the plane parallel to the Laponite surface despite the absence of strong water-Laponite hydrogen bonding, although again, in the direction perpendicular to the interface, no long range water ordering was found.[50-51] In this system the nanometer-thick Laponite particles had diameters of roughly 25 nm and a known crystalline structure. Studies on the NIMROD diffractometer at ISIS demonstrated that the water structures did not depend upon the sample age or aggregation state,[51] and that structural evolution of the material continued even after dynamical arrest, causing gelation, was reached. Using the small angle data the effects of sample aging upon the clay particle arrangement could be observed, causing changes in the slope of the differential cross section at small Q, and the growth of a signal in the older samples, in the range from 0.1 $Å^{-1} \leq Q \leq 1$ $Å^{-1}$, postulated to arise from edge-face clay particle contacts, since this corresponds to lengths between 6 and 60 Å, intermediate between the thickness and the diameter of a platelet.[50]

Atomistic analysis of this data however was restricted to the diffraction data in the range 0.5 $Å^{-1} \leq Q \leq 50$ $Å^{-1}$, due to the limits on available computational resources which mean that only a small part of a single Laponite platelet could fit into the EPSR simulation box. This restricted the analysis to the water-clay surface structures and water-water correlations rather than also allowing a full study of Laponite-Laponite particle interactions. Thus although data can currently be collected over wider length scales than has been previously available, limitations imposed by the need to undertake atomistic simulations on very large systems to cover these length scales mean computational resources are now a major factor that limits the applications in this area. For example, although the aforementioned NIMROD diffractometer can collect scattering data corresponding to pair correlation lengths of 300 Å, the current practical limit for atomistic modeling of these systems by EPSR is ~100Å at typical liquid-like system densities. On these achievable length scales, data processing times of one to two weeks can currently be delivered using typical desktop workstations, but as computer processors and efficient algorithms continue to be developed, this length scale of practicality will slowly increase.

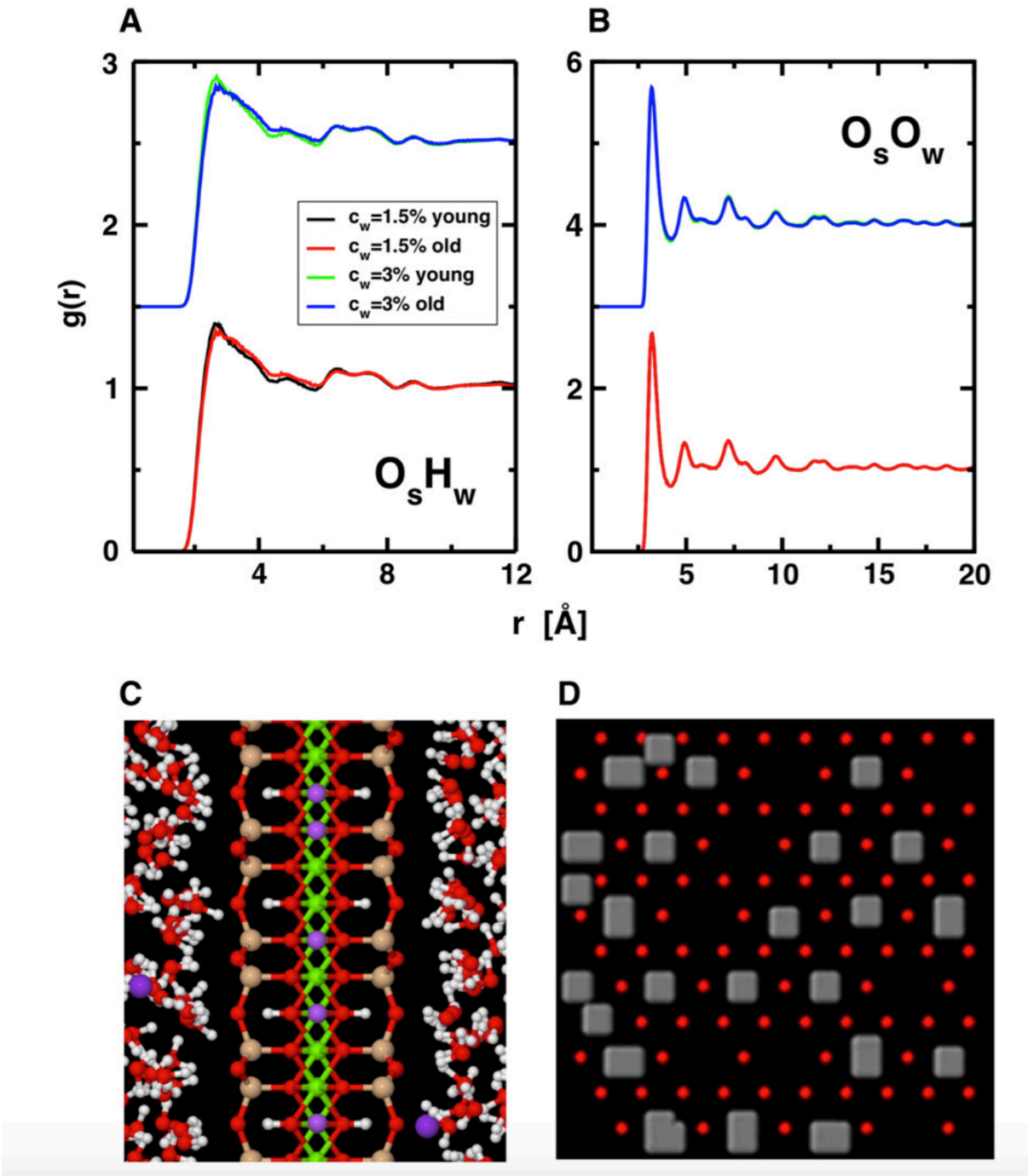

Figure 4: Radial Distribution Function of water atoms (Hw, Ow) relative to oxygen atoms on the Laponite surface (Os) showing A) OsHw and B) OsOw pairs for all four samples - two Laponite concentrations, 1.5 and 3wt% in water, freshly prepared (young) and aged (old). C) Snapshot of the central part of the EPSR simulation box showing the Laponite crystal in the middle (Os atoms in red) and the first layers of water molecules (Ow in red, Hw in white). All water molecules in the Laponite first neighbor layer orient their hydrogen atoms towards the Laponite surface. D) Red circles represent the Os spatial arrangement on the Laponite surface; the regions where the probability of finding a water molecule within 4 Å from the Laponite surface exceeds 20% is highlighted in gray. (Reprinted from Journal of Non-Crystalline Solids, M.A. Ricci, V. Tudisca, F. Bruni, R. Mancinelli, E. Scoppola, R. Angelini, B. Ruzicka, A.K. Soper, The structure of water near a charged crystalline surface, Vol 407, pages 418–422, Copyright (2015), with permission from Elsevier.)

The atomistic level study therefore limited analysis to the water structures found in the Laponite suspensions, which were found to be independent of clay concentration (from 1.5 to 3wt%) and aging time.[50-51] The samples were dilute so the water structure on the whole varied little from that found in pure bulk water, but the water layer close to the platelet surface was denser closer to the surface by a factor of 2, compared to the bulk, although this perturbation was limited to the first one or two water layers near the surface (Figure 4). The water molecules closest to the surface also demonstrated a strong polarization, arranged so that their molecular dipole moment pointed towards the Laponite surface, and arranged laterally on the surface so that they were located in the centre of the hexagons formed by surface oxygen sites on the Laponite. This arrangement resulted in long-range in-plane water ordering near the Laponite surface, as well as the higher density observed in this layer, without any requirement for strong H-bonding to the surface. The unusual water structuring in this system may ultimately help explain the long term aging behaviours seen in these systems, but needs to be combined with larger structural evolution data analysed from the same system.

Finally, wide angle diffraction has on one occasion been used to study structure in X-ray amorphous porous biogenic iron sulphide nanoparticles, alongside small angle neutron scattering and EXAFS data probing Fe-S bonding.[52] SANS data demonstrated an average particle diameter of around 2nm while the wide-angle scattering and EXAFS data suggested the presence of shells of 3 S around a central Fe and further shells containing Fe at further distances from the central atom. In materials such as these the use of both wide and small angle scattering combined with isotopic substitution in the surrounding solvent could now assist in determining both the nanoparticle size and porosity in addition to any potential ordering of the inorganic phase. Since wide and small angle data can now be collected simultaneously on such samples, rather than having to use separate instruments, data collection will be facilitated enabling more detailed studies of such materials. However limitations remain imposed by currently available computational power, and the necessary size of atomistic simulations needed to fit multiple contrast data of this type.

6. Summary

The application of wide angle scattering to materials and systems containing nanometric ordering normally studied with small angle scattering has been recently enhanced by advances both in experimental instrumentation and the available computational tools and resource

available to analyse the data. These new experimental studies, that provide high-resolution structural information, are rapidly opening up new perspectives on colloidal and soft matter systems. For example, this detailed insight into atomic and molecular interactions is slowly transforming our understanding of many fundamental phenomena for which atomistic theories have largely been lacking e.g. the driving forces for hydrophobic interactions between non-polar moieties in aqueous solution, and the complex distribution of ions in the electrical double-layer that stabilizes colloidal suspensions and hydrated clay structures. Ultimately this new insight into the atomistic underpinnings of complex systems should allow us to optimize our ability to control chemical processes on molecular length scales and consequently realize our full potential for engineering the plethora of nano-scale materials that are required for many modern technological advances.

References: (highlighted papers listed at end)

1. Feigin, L.; Svergun, D. I.; Taylor, G. W., *Structure analysis by small-angle X-ray and neutron scattering*. Springer: 1987.
2. Glatter, O.; Kratky, O., *Small Angle X-ray Scattering*. Academic Press: London, 1982.
3. Pedersen, J. S., Analysis of small-angle scattering data from colloids and polymer solutions: Modeling and least squares fitting. *Adv. Colloid Interface Sci.* **1997,** *70*, 171-210.
4. Hayter, J. B.; Penfold, J., Determination of micelle structure and charge by neutron small-angle scattering. *Colloid & Polymer Sci* **1983,** *261* (12), 1022-1030.
5. O'Driscoll, B. M. D.; Milsom, E.; Fernandez-Martin, C.; White, L.; Roser, S. J.; Edler, K. J., Thin Films of Polyethylenimines and Alkyltrimethylammonium Bromides at the Air/Water Interface. *Macromol.* **2005,** *38* (21), 8785-8794.
6. Keen, D., A comparison of various commonly used correlation functions for describing total scattering. *J. Appl. Cryst.* **2001,** *34* (2), 172-177.
7. Faber, T. E.; Ziman, J. M., A theory of the electrical properties of liquid metals. *Philosophical Magazine* **1965,** *11* (109), 153-173.
8. McGreevy, R. L., Reverse Monte Carlo modelling. *J. Phys.: Condens. Matter* **2001,** *13* (46), R877.
9. Soper, A. K., Empirical potential Monte Carlo simulation of fluid structure. *Chem. Phys.* **1996,** *202* (2–3), 295-306.
10. Soper, A. K., Partial structure factors from disordered materials diffraction data: An approach using empirical potential structure refinement. *Phys. Rev. B* **2005,** *72* (10), 104204.

11. Heenan, R. K.; Rogers, S. E.; Turner, D.; Terry, A. E.; Treadgold, J.; King, S. M., Small Angle Neutron Scattering Using Sans2d. *Neutron News* **2011,** *22* (2), 19-21.
12. Benmore, C. J.; Soper, A. K., The SANDALS manual: a Guide to Performing Experiments on the Small Angle Neutron Diffractometer for Amorphous and Liquid Samples at ISIS. . *Rutherford Appleton Laboratory Technical Report* **1998**, RAL-TR-1998-006.
13. Bowron, D. T.; Soper, A. K.; Jones, K.; Ansell, S.; Birch, S.; Norris, J.; Perrott, L.; Riedel, D.; Rhodes, N. J.; Wakefield, S. R.; Botti, A.; Ricci, M.-A.; Grazzi, F.; Zoppi, M. , NIMROD: The Near and InterMediate Range Order Diffractometer of the ISIS second target station. *Rev. Sci. Instru.* **2010,** *81*, 033905.
14. Bowron, D. T.; Finney, J. L., Association and Dissociation of an Aqueous Amphiphile at Elevated Temperatures. *J. Phys. Chem. B* **2007,** *111* (33), 9838-9852.
15. Dixit, S.; Crain, J.; Poon, W. C. K.; Finney, J. L.; Soper, A. K., Molecular segregation observed in a concentrated alcohol-water solution. *Nature* **2002,** *416* (6883), 829-832.
16. Dixit, S.; Soper, A. K.; Finney, J. L.; Crain, J., Water structure and solute association in dilute aqueous methanol. *EPL (Europhysics Letters)* **2002,** *59* (3), 377.
17. Dougan, L.; Bates, S. P.; Hargreaves, R.; Fox, J. P.; Crain, J.; Finney, J. L.; Réat, V.; Soper, A. K., Methanol-water solutions: A bi-percolating liquid mixture. *J. Chem. Phys.* **2004,** *121* (13), 6456-6462.
18. Dougan, L.; Hargreaves, R.; Bates, S. P.; Finney, J. L.; Réat, V.; Soper, A. K.; Crain, J., Segregation in aqueous methanol enhanced by cooling and compression. *J. Chem. Phys.* **2005,** *122* (17), 174514.
19. Soper, A. K.; Dougan, L.; Crain, J.; Finney, J. L., Excess Entropy in Alcohol−Water Solutions: A Simple Clustering Explanation†. *J. Phys. Chem. B* **2006,** *110* (8), 3472-3476.
20. Dougan, L.; Crain, J.; Finney, J. L.; Soper, A. K., Molecular self-assembly in a model amphiphile system. *Phys. Chem. Chem. Phys.* **2010,** *12* (35), 10221-10229.
21. Frank, H. S.; Evans, M. W., Free Volume and Entropy in Condensed Systems III. Entropy in Binary Liquid Mixtures; Partial Molal Entropy in Dilute Solutions; Structure and Thermodynamics in Aqueous Electrolytes. *J. Chem. Phys.* **1945,** *13* (11), 507-532.
22. Bowron, D. T.; Moreno, S. D., Structural correlations of water molecules in a concentrated alcohol solution. *J. Phys: Condens. Matter* **2003,** *15* (1), S121.
23. Bowron, D. T.; Moreno, S. D. a., The structure of a concentrated aqueous solution of tertiary butanol: Water pockets and resulting perturbations. *J. Chem. Phys.* **2002,** *117* (8), 3753-3762.

24. Chou, S. G.; Soper, A. K.; Khodadadi, S.; Curtis, J. E.; Krueger, S.; Cicerone, M. T.; Fitch, A. N.; Shalaev, E. Y., Pronounced Microheterogeneity in a Sorbitol–Water Mixture Observed through Variable Temperature Neutron Scattering. *J. Phys. Chem. B* **2012,** *116* (15), 4439-4447.

25. Bowron, D. T.; Díaz Moreno, S., The Structure of a Trimolecular Liquid: tert-Butyl Alcohol:Cyclohexene:Water. *J. Phys. Chem. B* **2005,** *109* (33), 16210-16218.

26. Deetlefs, M.; Hardacre, C.; Nieuwenhuyzen, M.; Padua, A. A. H.; Sheppard, O.; Soper, A. K., Liquid Structure of the Ionic Liquid 1,3-Dimethylimidazolium Bis{(trifluoromethyl)sulfonyl}amide. *J. Phys. Chem. B* **2006,** *110* (24), 12055-12061.

27. Hardacre, C.; Holbrey, J. D.; McMath, S. E. J.; Bowron, D. T.; Soper, A. K., Structure of molten 1,3-dimethylimidazolium chloride using neutron diffraction. *J. Chem. Phys.* **2003,** *118* (1), 273-278.

28. Hayes, R.; Imberti, S.; Warr, G. G.; Atkin, R., Amphiphilicity determines nanostructure in protic ionic liquids. *Phys. Chem. Chem. Phys.* **2011,** *13* (8), 3237-3247.

29. Canongia Lopes, J. N. A.; Pádua, A. A. H., Nanostructural Organization in Ionic Liquids. *J. Phys. Chem. B* **2006,** *110* (7), 3330-3335.

30. Hardacre, C.; Holbrey, J. D.; Mullan, C. L.; Youngs, T. G. A.; Bowron, D. T., Small angle neutron scattering from 1-alkyl-3-methylimidazolium hexafluorophosphate ionic liquids ([Cnmim][PF6], n=4, 6, and 8). *J. Chem. Phys.* **2010,** *133* (7), -.

31. Hayes, R.; Imberti, S.; Warr, G. G.; Atkin, R., How Water Dissolves in Protic Ionic Liquids. *Angew. Chem. Intl Ed.* **2012,** *51* (30), 7468-7471.

32. Shashkov, S. N.; Kiselev, M. A.; Tioutiounnikov, S. N.; Kiselev, A. M.; Lesieur, P., The study of DMSO/water and DPPC/DMSO/water system by means of the X-ray, neutron small-angle scattering, calorimetry and IR spectroscopy. *Physica B: Condens. Matter* **1999,** *271* (1–4), 184-191.

33. Kiselev, M. A.; Lesieur, P.; Kisselev, A. M.; Grabielle-Madelmond, C.; Ollivon, M., DMSO-induced dehydration of DPPC membranes studied by X-ray diffraction, small-angle neutron scattering, and calorimetry. *J. Alloys Compounds* **1999,** *286* (1–2), 195-202.

34. Yu, Z. W.; Quinn, P. J., Phase stability of phosphatidylcholines in dimethylsulfoxide solutions. *Biophys. J.* **1995,** *69* (4), 1456-1463.

35. Dabkowska, A. P.; Foglia, F.; Lawrence, M. J.; Lorenz, C. D.; McLain, S. E., On the solvation structure of dimethylsulfoxide/water around the phosphatidylcholine head group in solution. *J. Chem. Phys.* **2011,** *135* (22), 225105.

36. Dabkowska, A. P.; Lawrence, M. J.; McLain, S. E.; Lorenz, C. D., On the nature of hydrogen bonding between the phosphatidylcholine head group and water and dimethylsulfoxide. *Chem. Phys.* **2013,** *410* (0), 31-36.

37. Mason, P. E.; Neilson, G. W.; Kline, S. R.; Dempsey, C. E.; Brady, J. W., Nanometer-Scale Ion Aggregates in Aqueous Electrolyte Solutions: Guanidinium Carbonate. *J. Phys. Chem. B* **2006,** *110* (27), 13477-13483.

38. Hunger, J.; Niedermayer, S.; Buchner, R.; Hefter, G., Are Nanoscale Ion Aggregates Present in Aqueous Solutions of Guanidinium Salts? *J. Phys. Chem. B* **2010,** *114* (43), 13617-13627.

39. Troitzsch, R. Z.; Martyna, G. J.; McLain, S. E.; Soper, A. K.; Crain, J., Structure of Aqueous Proline via Parallel Tempering Molecular Dynamics and Neutron Diffraction. *J. Phys. Chem. B* **2007,** *111* (28), 8210-8222.

40. McLain, S. E.; Soper, A. K.; Terry, A. E.; Watts, A., Structure and Hydration of l-Proline in Aqueous Solutions. *J. Phys. Chem. B* **2007,** *111* (17), 4568-4580.

41. Rhys, N. H.; Soper, A. K.; Dougan, L., The Hydrogen-Bonding Ability of the Amino Acid Glutamine Revealed by Neutron Diffraction Experiments. *J. Phys. Chem. B* **2012,** *116* (45), 13308-13319.

42. Hargreaves, R.; Bowron, D. T.; Edler, K. J., The atomistic structure of a micelle in solution determined by wide Q-range neutron diffraction. *J. Am. Chem. Soc.* **2011,** *133* (41), 16524-16536.

43. Dorrance, R. C.; Hunter, T. F., Absorption and emission studies of solubilization in micelles. Part 2.-Determination of aggregation numbers and solubilisate diffusion in cationic micelles. *J. Chem. Soc., Faraday Trans. 1* **1974,** *70* (0), 1572-1580.

44. Yoshida, N.; Matsuoka, K.; Moroi, Y., Micelle Formation of n-Decyltrimethylammonium Perfluorocarboxylates. *J. Colloid Interface Sci.* **1997,** *187* (2), 388-395.

45. D'Errico, G.; Ortona, O.; Paduano, L.; Vitagliano, V., Transport Properties of Aqueous Solutions of Alkyltrimethylammonium Bromide Surfactants at 25°C. *J. Colloid Interface Sci.* **2001,** *239* (1), 264-271.

46. Hayter, J. B., A self-consistent theory of dressed micelles. *Langmuir* **1992,** *8* (12), 2873-2876.

47. Mancinelli, R.; Bruni, F.; Ricci, M. A.; Imberti, S., Microscopic structure of water in a water/oil emulsion. *J. Chem. Phys.* **2013,** *138* (20), 204503.

48. Tombari, E.; Ferrari, C.; Salvetti, G.; Johari, G. P., Water↔ice transformation in micron-size droplets in emulsions. *J. Chem. Phys.* **1999,** *111* (7), 3115-3120.
49. Williams, G. D.; Soper, A. K.; Skipper, N. T.; Smalley, M. V., High-Resolution Structural Study of an Electrical Double Layer by Neutron Diffraction. *J. Phys. Chem. B* **1998,** *102* (45), 8945-8949.
50. Tudisca, V.; Bruni, F.; Scoppola, E.; Angelini, R.; Ruzicka, B.; Zulian, L.; Soper, A. K.; Ricci, M. A., Neutron diffraction study of aqueous Laponite suspensions at the NIMROD diffractometer. *Phys. Rev. E* **2014,** *90* (3), 032301.
51. Ricci, M. A.; Tudisca, V.; Bruni, F.; Mancinelli, R.; Scoppola, E.; Angelini, R.; Ruzicka, B.; Soper, A. K., The structure of water near a charged crystalline surface. *J. Non-Cryst. Solids* **2015,** *407* (0), 418-422.
52. Watson, J. H. P.; Ellwood, D. C.; Soper, A. K.; Charnock, J., Nanosized strongly-magnetic bacterially-produced iron sulfide materials. *J. Magnetism Magnetic Mater.* **1999,** *203* (1–3), 69-72.

Highlighted References:

Reference 10 (Soper PRB 2005) Describes the EPSR methodology which gives the ability to comprehend the experimental data on the structural correlations that underpin complex liquid systems.

Reference 13 (Bowron Rev Sci Inst. 2010) Describes NIMROD the near and intermediate range order diffractometer at ISIS which is delivering transformative experimental capability by bridging the traditional gap between SANS and wide-angle neutron scattering.

Reference 15 (Dixit Nature 2002) Demonstrates that microheterogenieties are a fundamental aspect of solutions that are in general considered "well mixed".

Reference 28 (Hayes PCCP 2011) A very nice description of the structure of room temperature ionic liquids in terms of an analogy with a foam or emulsion like description of the molecular ion ordering.

Reference 42 (Hargreaves JACS 2011) First study of large molecular aggregates in solution using wide angle scattering data, demonstrating the utility of this technique for obtaining high resolution structures of complex molecular systems.

Reference 47 (Mancinelli JCP 2013) First application of wide-angle scattering techniques to water confinement by soft structures.

Reference 49 (Williams JPCB 1998) First study of electrical double layer structure near clay surfaces using wide angle neutron scattering, with the unexpected result that the counterions were not bound to the clay surface in the Stern layer but were instead located in midplane of the interlayer spacing.

Reference 50 (Tudisca PRE 2014) A very clearly described analysis of water structure near Laponite surfaces, including a description of the corrections required for low angle data arising from inelastic scattering and multiple scattering contributions to the measured signal.